EMRP
European Metrology Research Programme
Programme of EURAMET

The EMRP is jointly funded by the EMRP participating countries within EURAMET and the European Union

Deliverable Number	4.1.9	**Lead Partner**	**PTB**
Deliverable Title	Photoelectron spectroscopy on organic semiconductors		
Contractual Delivery Date	Jun 17	**Deliverable type**	Good Practice guide
Actual Delivery Date	Jun 17	**Contributors**	

Deliverable Details

Good Practice guide – Photoelectron spectroscopy on organic semiconductors

1 Introduction

A relevant method for the investigation of organic compounds relevant for photovoltaic devices is photoelectron spectroscopy (UPS - Ultraviolet photoelectron spectroscopy and XPS - X-ray photoelectron spectroscopy). In this good practice guide the preparation of samples, the calibration of the energy scale of the XP spectra as well as the measurement conditions and evaluation procedure are described.

2 Photoelectron Spectroscopy - PES

2.1 Physical principle

XPS is based on the photoelectric effect. When a sample surface is irradiated with photons (Fig. 1), an incident photon of energy $h\nu$ can be absorbed by an electron with binding energy E_B below the vacuum level: the entire photon energy is transferred to the electron, which is then promoted to an unoccupied state above the vacuum level. As a result, this photoelectron is ejected from the sample to the vacuum with kinetic energy: $E_{kin} = h\nu - E_B \quad (1)$ and can be detected by an electron energy analyzer.

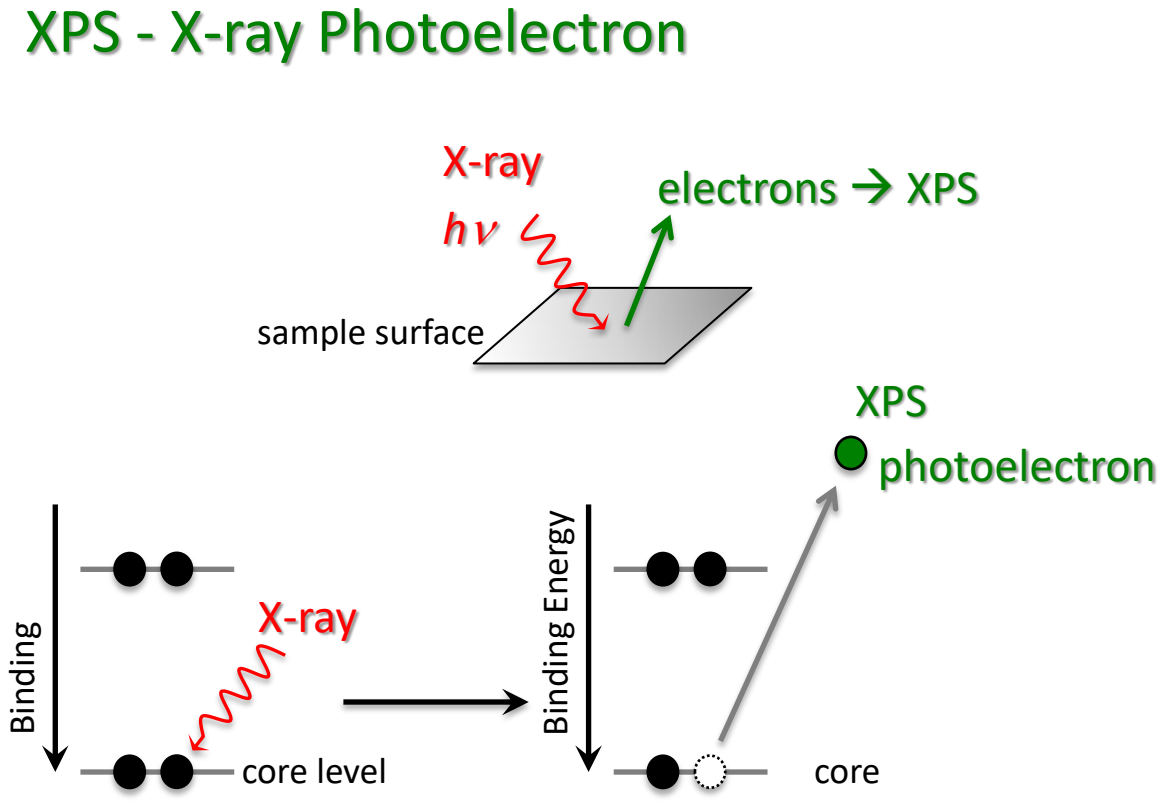

Figure 1: principle of photoelectron evolution

For a solid surface the binding energy (E_b) is usually measured with respect to the Fermi level and the equation is written in the form:

$$E_{kin} = h\nu - E_b - \Phi_w \quad (2)$$

Here, Φ_w is the work function of the sample's material and represents the minimum energy required to remove an electron from the sample. To excite an electron, the photon energy must be greater than E_b with the difference at least exceeding Φ_w.

In this simplified single particle picture based on a single electron being excited, it is clear that the energy distribution of photoemitted electrons should represent the electron states in the sample shifted up in energy by an amount $h\nu - \Phi_w$ (see Fig. 2). In reality, it provides a distorted replica of the electronic structure, influenced by the occurrence of multi-electron processes and by the fact that the probability of a photon being absorbed is not the same for all electron states. The ejected electrons can originate from core levels or from the occupied part of the valence band (Fig. 2). Due to the relatively high photon energy (typically in the range between 100 eV and 2000 eV), XPS is focused on core level electrons whereas UPS with lower photon energies is focused on the valence band.

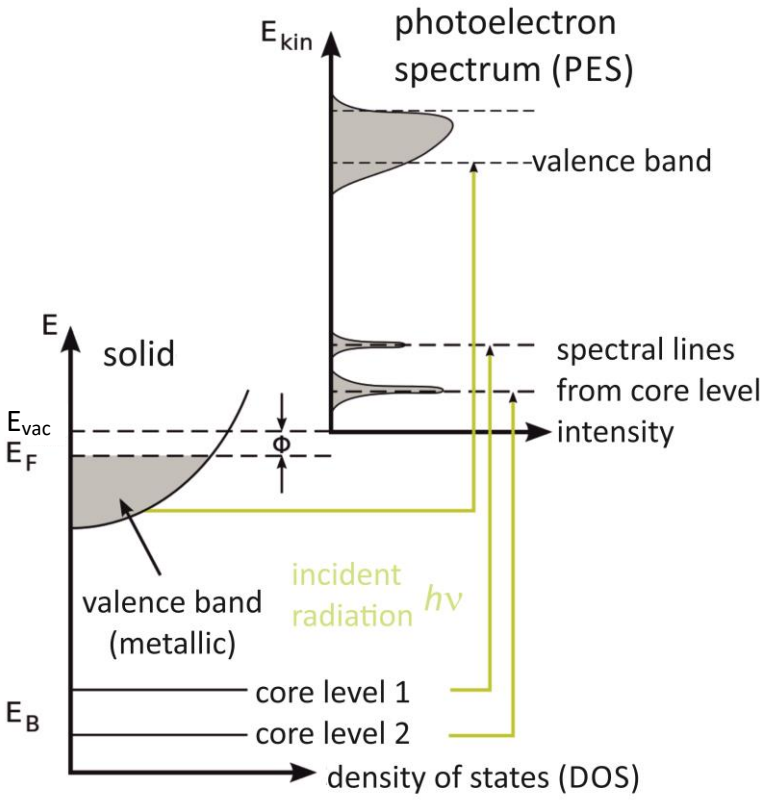

Figure 2: Scheme of the photoemission process (simple picture)). The photoelectron distribution can be measured by an electron energy analyzer.

The following aspects of XPS need further attention:

- the elemental sensitivity
- the chemical state specificity
- the surface sensitivity

1. A typical XPS spectrum is obtained at a given photon energy by recording the number of photoelectrons in dependence of their kinetic energy and is plotted as a function of the binding energy by making use of Eq. (2). The spectrum reflects the sequence of occupied levels - in particular the core levels - in the sample. Since the binding energies of core levels are different for (and therefore characteristic of) each chemical element, and no two elements share the same set of binding energies, photoemission spectra can serve as fingerprints of the respective elements.

For example, a peak located at E_b = 285 eV is characteristic of photoelectrons coming from the C 1s core level, while the O 1s photoemission line appears at higher binding energy (E_b ≈ 532 eV). This elemental sensitivity is one reason to employ PES as a very useful analytical tool, making it possible - for instance - to determine the composition of unknown samples and to get an information about the cleanliness of solid surfaces. XPS can be used for analysis of all elements in the periodic table except hydrogen and helium.

2. When comparing the binding energies of core electrons of a given element in different chemical environments (i.e., in different molecules, compounds or solids), it becomes evident that the exact value of E_b depends on the chemical environment of the atoms and that energy shifts may occur when inequivalent atoms of the same elemental species are present (Fig. 3). These shifts in the energetic position in the spectrum are called chemical shifts. In general, electrons photoemitted from atoms in a higher positive oxidation state appear at a higher binding energy because of the increased Coulomb interaction with the ion core upon withdrawal of valence charge due to chemical bonding.

In figure 3 two spectra of mixtures of different carbon species are shown. Due to different bonds the carbon peak is shifted for the various species in the spectrum.

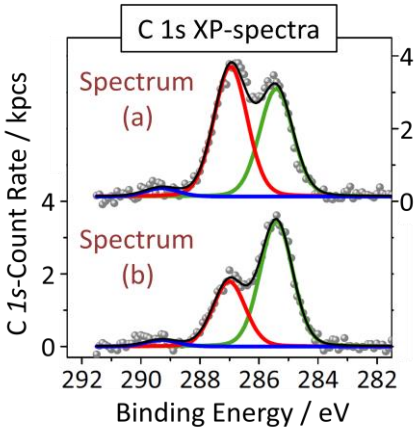

Figure 3: chemical shift of carbon peak for different species in spectra (a) and (b)

By comparison with data from qualified reference substances or available databases, the values of the binding energy shifts can often be used to determine oxidation states and to gain insight into the nature of the chemical bond formed by the atoms. This chemical state specificity represents the power of XPS for application in chemistry, surface physics and materials research. This is why XPS is also known as ESCA (Electron Spectroscopy for Chemical Analysis).

3. Due to the strong interaction of electrons with matter, XPS and all electron spectroscopies are very surface sensitive. The electrons travelling in a solid exhibit a very short inelastic mean free path, λ_e. This quantity describes the average distance an electron can travel within the material without suffering energy losses by inelastic scattering; it indicates the electron escape depth. For electrons with kinetic energy in the range between 10 eV and 1000 eV, λ_e can vary between 0.5 nm and 3 nm

depending on the material [Seah and Dench, 1979 Surf. and Interf. Anal. 1(1) 2-11]. This results in a thickness of only a few atomic layers. As a result, in a typical photoemission experiment only electrons originating from a region at the solid-vacuum interface can reach the detector without losing energy, thus contributing to the main lines of the measured spectrum. Hence, PES and XPS are widely employed to probe the electronic structure and composition of solid surfaces and thin films.

2.2 Decay of a core hole

The ejection of an electron from an inner shell creates an electronically excited state with a core hole in that shell. This excited state can decay via two distinct routes:

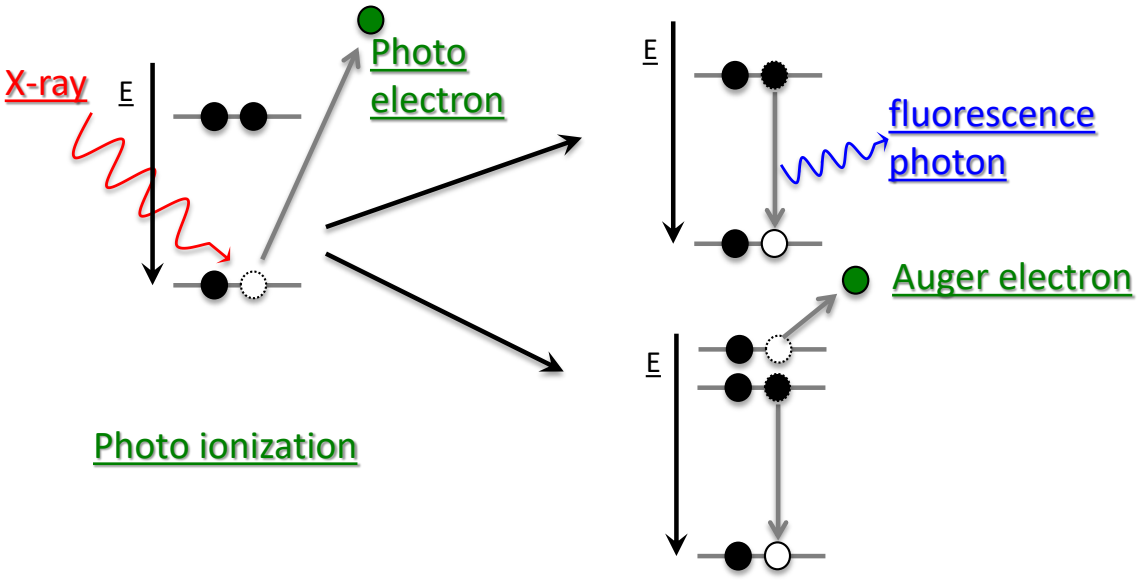

Figure 4: Schematic of X-ray fluorescence and Auger decay following a photoionization

- The core hole is filled by an electron from an outer shell with simultaneous emission of a photon with energy equal to the difference in binding energy of the two levels involved in the electron transition. This is the X-ray emission process or X-ray fluorescence (Fig. 4, upper path).
- The core hole is filled by an electron from an outer shell, but the excess energy is transferred to another outer shell electron, which is emitted (Fig. 4, lower path). The process, called Auger decay, involves three electrons: the electron knocked out in the initial photoionization event, the electron that decays to fill the inner shell vacancy, and the emitted electron from the outer shell (Auger electron). As a consequence, the final state is a doubly ionized state.

X-ray fluorescence and Auger electron emission are competitive processes; the probability of each is given by the respective decay cross-sections. For binding energies below 1.5 keV, as in the present experiment, and especially for elements with low atomic number, the non-radiative decay prevails.

2.3 Linewidth of core level lines

The width and shape of a photoemission peak in the spectrum results from the convolution of different effects. An important contribution is related to instrumental factors, primarily the linewidth and lineshape of the X-ray line used for the excitation and the resolution of the electron energy analyzer employed to analyze the spectral distribution of photoelectrons. A further contribution is related to the photoemission process itself. It is the peak broadening due to the finite lifetime of the core hole. Also thermal broadening by coupling with intra-molecular vibrations and phonons might

be included in some cases. Many-body effects, such as the excitation of electron-hole pairs close to the Fermi level in metals or shake-up satellites that cannot be resolved due to limited instrumental resolution, can cause additional asymmetric broadening with a tail on the low kinetic energy side of the photoemission peak.

Instrumental and vibrational broadening yield in Gaussian line shapes. The spectral line shape due to the core-hole-lifetime τ follows a Lorentzian function with full-width at half-maximum (FWHM) 2Γ, the intrinsic or natural linewidth, which is related to the mean lifetime through the relationship [J. J. Sakurai, Modern Quantum Mechanics, Addison-Wesley Publishing Company, Reading - Massachusetts, 1995. 341-345.]:

$$2\Gamma = \frac{\hbar}{\tau} = \frac{6.58 \cdot 10^{-16}\text{eVs}}{\tau} \qquad (3)$$

2 Γ is typically larger for inner shell orbitals, as these can be filled rapidly by electrons from outer shells. Therefore, for a given element 2 Γ tends to increase with increasing binding energy. Similarly, for a given core level orbital (e.g., 1s) 2 Γ increases as the atomic number Z increases, due to the higher valence electron density in atoms with higher Z.

The contributions of intrinsic and instrumental effects to the experimentally observed linewidth can be combined in a first approximation into a quadratic sum [B. D. Ratner and D. G. Castner, Electron Spectroscopy for Chemical Analysis (Chapter4), in: Surface Analysis | The Principal Techniques, edited by J. C. Vickerman, J. Wiley & Sons Ltd., 1997]:

$$\text{FWHM}_{\text{tot}}^2 = (2\Gamma)^2 + \text{FWHM}_{\text{X}}^2 + \text{FWHM}_{\text{A}}^2 \qquad (4)$$

with the second and third term on the right side including the X-ray source and analyzer energy resolution.

2.4 Spin-orbit splitting of core level lines

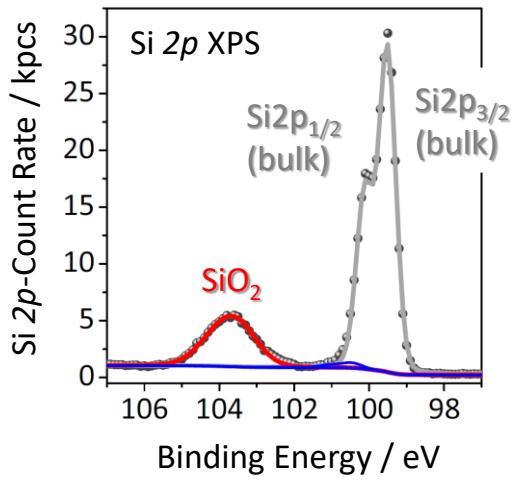

Figure 5: Spin-orbit coupling leads to a splitting of the 2p photoemission line of silicon into a doublet

In the photoemission from p, d and f inner subshells the spectral lines are split into two component peaks (Fig. 5). This splitting arises from spin-orbit coupling effects in the final state [B. D. Ratner and D. G. Castner, Electron Spectroscopy for Chemical Analysis (Chapter 4), in: Surface Analysis | The Principal Techniques, edited by J. C. Vickerman, J. Wiley & Sons Ltd., 1997]. While in the initial state the inner subshells are completely filled (for example, the configuration of the inner shells in silicon is: (1s)2 (2s)2 (2p)6 (3s)2 (3p)2, in the final state one electron has been removed and an unpaired spin is left behind. The spin can be oriented up or down, and if the core hole belongs to an orbital with non-zero orbital angular momentum (l > 0) there will be a coupling between the unpaired spin and the orbital angular momentum: the two states $j+ = l + 1/2$ and $j- = l - 1/2$ are not degenerate and a spin-orbit split doublet is observed

in the photoelectron spectrum. The intensity ratio of the two spin-orbit components is dictated by the ratio of the respective multiplicities:

$(2j_+ + 1)/(2j_- + 1) = (2l + 2)/2l$, which determines the relative probability of transition to the two states upon photoionization. In general, in the photoemission spectrum from a given subshell the core level subpeak with maximum j is detected at lower binding energy. Obviously, no spin-orbit splitting occurs in the photoemission from s core levels.

2.5 Summary - spectral features in a photoemission spectrum

The main spectral features that can be observed in a typical XPS spectrum of a solid (as the one illustrated in Fig. 6) and reflect the characteristic excitation processes in condensed matter are described so far.

As written before, XPS spectra are in general dominated by sharp peaks corresponding to core level photoemission. These peaks may be (partially) chemically shifted and be spin-orbit split. Their binding energies always incorporate the contribution of the relaxation shift and their linewidth can be affected by many-body effects, instrumental resolution and natural broadening. From the relative intensity of core level peaks one can estimate semi-quantitatively elemental ratios, in order to assess the relative surface coverage of adsorbates and contaminants or the stoichiometry of a compound. To do so, it is necessary to correct the relative intensities by the respective photoionization cross-sections, which express the probability of creating a photoelectron in each core level at the photon energy $h\nu$.

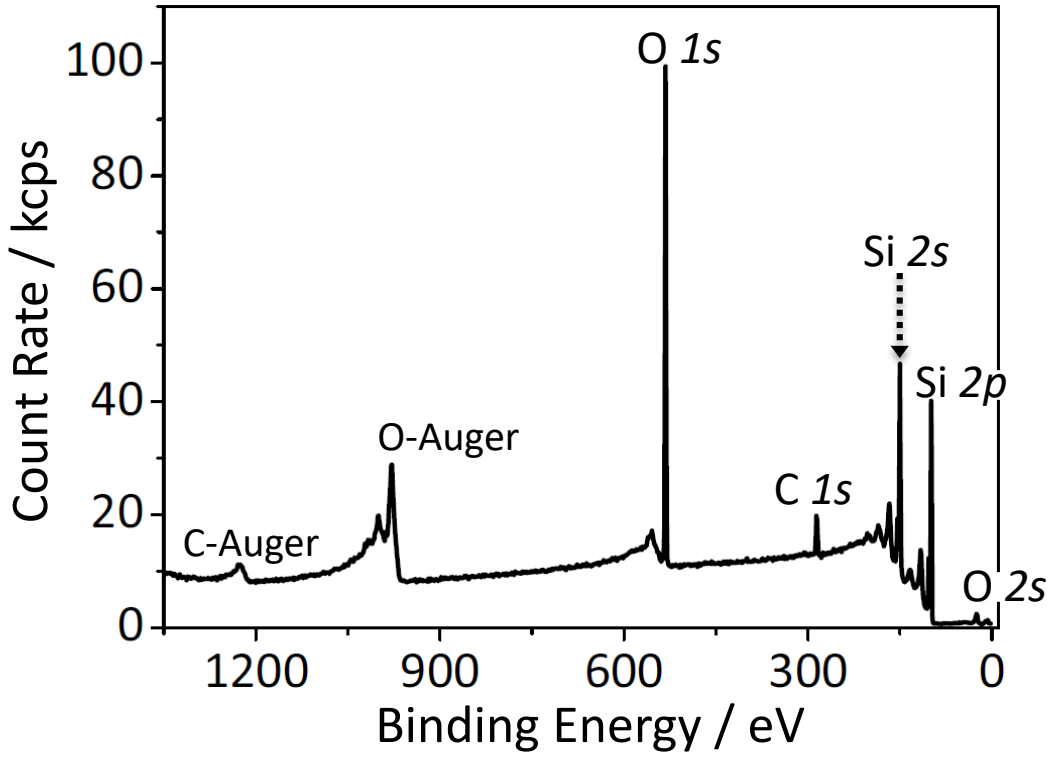

Figure 6: A typical XPS overview spectrum from a solid surface (here silicon).

Besides the core level lines, electron emission from the valence band is observed. This part of the spectrum represents a projection of the occupied electronic states, and the photoemission intensity drops to zero above the Fermi level (Fig. 6, lower binding energy end of the spectrum).

As all electrons emitted from the sample are detected by the electron energy analyzer, Auger lines are often observed. If it is possible to change the photon energy of the incident radiation, an Auger line can be easily distinguished from a core level line. Auger electrons appear at fixed kinetic energy regardless of the photon energy in contrast to photoelectrons, the spectral position of which moves with the photon energy according to Eq. (2).

Satellites corresponding to multi-electron excitations, such as multiple plasmon losses and shake-up satellites, may be also visible in the XPS overview spectrum. All photoemission features appear superimposed on a featureless background, arising from inelastically scattered electrons (which undergo energy losses before escaping from the surface) and secondary electrons excited in "cascade" processes.

2.6 Sampling depth of XPS and collection geometry

As written in section 2.1, XPS is very surface sensitive due to the short inelastic mean free path of electrons. While X-rays interact only weakly with matter and can penetrate deeper into a solid (1000 nm or more at $h\nu = 1$ keV), electrons with energy in the range 5-1500 eV lose energy by inelastic scattering. The XPS experiments are mainly concerned with the intensity of emitted photoelectrons that have suffered no energy losses. Therefore, the XPS sampling depth refers to a characteristic length over which electrons can travel without undergoing inelastic scattering events. This quantity is the inelastic mean free path λ_e, which is defined as the average distance that an electron of given kinetic energy E_{kin} travels between two successive inelastic collisions [B. D. Ratner and D. G. Castner, Electron Spectroscopy for Chemical Analysis (Chapter 4), in: Surface Analysis | The Principal Techniques, edited by J. C. Vickerman, J. Wiley & Sons Ltd., 1997.]. The probability that the electron travels a distance *z* through the solid without undergoing inelastic scattering can be written as an exponential decay:

$$P(z) \propto e^{-\frac{z}{\lambda_e}} \Rightarrow \langle z \rangle = \int zP(z)dz = \lambda_e \tag{5}$$

Considering the electrons emitted in the direction perpendicular to a solid surface, a small element of thickness *dz* at a distance *z* from the surface (*z* = 0 denotes the surface plane) will give a contribution *dI* to the measured intensity:

$$dI \propto e^{-\frac{z}{\lambda_e}}dz \tag{6}$$

The total intensity *I*, coming from a thin film of thickness *t* right underneath the surface, is obtained by integrating Eq. (6) between 0 and *t*, and it thus amounts to:

$$I = I_0\left[1 - e^{-\frac{t}{\lambda_e}}\right] \tag{7}$$

The sampling depth of the XPS experiment is often defined as $t = 3\lambda_e$, which means that 95% of the photoemission intensity of the core level line comes from the corresponding region ($3\lambda_e$ thick) below the surface.

When detecting photoelectrons emitted at an angle θ_e away from the surface normal (see Fig. 1a), one has to consider the effective path $z/\cos\theta_e$ of the electrons in the solid, and Eq. (6) becomes:

$$dI \propto \exp\left[-\frac{z}{\lambda_e \cdot \cos\theta_e}\right] dz \qquad (8)$$

In grazing emission geometry the sampling depth is reduced to $3\lambda_e \cos\theta_e$ and the surface sensitivity of the measurements is strongly increased (e.g., $\theta_e = 80° \Rightarrow \cos\theta_e \sim 0.17$).

3 Instrumentation

This good practice guide is based on measurements carried out at an electron storage ring. The instrumentation (Fig. 7) for the UPS measurements is placed at PTB's electron storage ring the Metrology Light Source (MLS) in Berlin.

The spectra were taken at the insertion device beamline (IDB) at the MLS. This beamline uses an U125 undulator (125 mm period length) as radiation source, and a plane grating monochromator capable to cover a photon energy range between 280 eV (λ = 4.42 nm) and 1.55 eV (λ = 800 nm) by different optical configurations.

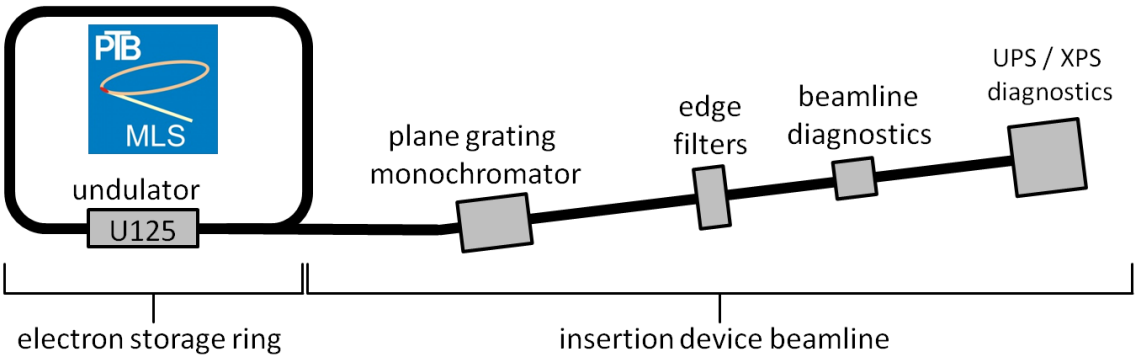

Figure 7: Schematic illustration of the experimental setup of the insertion device beamline (IDB) at the Metrology Light Source (MLS).

The beamline diagnostic unit consists of different intensity monitors (photoemission detector, calibrated photodiodes) which can be put into the beam, if required to determine the radiation power. The experimental setup can be attached to a preparation chamber which enables to carry out various processes and their characterization by UPS/XPS in situ, i.e. analysis and preparation of the samples can take place in the same vacuum chamber without exposing the sample to atmosphere.

To investigate thin film surfaces UPS and XPS were employed using the iDEEAA instrumentation [C. Lupulescu et al., J. Electr. Spectr. Rel. Phen. (2013) 191, 104]. The iDEEAA spectrometer is equipped with a Scienta R4000 hemispherical electron analyzer operated at a pass energy of 100 eV. The angle between surface normal and electron spectrometer was 45°. For the measurements intended by this document excitation energies of 125 eV for valence band (VB) spectra and of 200 eV for S 2p core level measurements are best suited while employing radiation from a synchrotron. To compare the VB spectra they are to be normalized at the count rate at a Binding Energy(BE) of 40 eV, which is above the electronic structure relevant for the VB spectra.

The transmission function *T(KE)* of the electron spectrometer is a parameter predominantly influenced by the instrumentation. We determined the *T(KE)* of the electron analyzer for a pass energy of 40 eV by measuring Cu, Ag, Au, and Ge reference samples with the QPA method described in detail by Hesse et al. [Hesse R, Streubel P, Szargan R 2005 Improved accuracy of quantitative XPS analysis using predetermined spectrometer transmission functions with UNIFIT 2004 Surf. Interface Anal. 37 589-607].

Normal emission geometry was used for XPS measurements, whereas the surface of the sample was perpendicular to the entrance slit of the electron analyser and the incoming photons hit the sample under 6°. The electron analyser was operated at two different pass energies (80 eV for the survey and 40 eV for higher resolution scans of peaks of interest). To correct unintentional energy shifts, e.g. due to positive charging effects, the binding energy scale of the XP spectra was referenced to the Si 2p3/2 signal of the bulk silicon at *BE* = 99.5 eV.

A pass energy of 40 eV was used for C 1s, O 1s, F 1s and S 2p core level spectra and 80 eV for survey spectra. For all XPS measurements at the ARGUS CU instrumentation, monochromatized Al-Kα radiation was used for excitation. The angle between surface normal and electron spectrometer was 0° and the angle between surface normal and X-ray source was 54.7°

The binding energy (*BE*) scales of both photoelectron spectrometers were referenced to the Au 4f7/2 signal of a cleaned Au sample [2].

4 Sample preparation

As example two polymer and three molecular organic compounds relevant for organic solar cells were measured for this document (Fig. 8). Both polymers (PTB7 and MEH-PPV) were deposited by spin coating onto an ITO coated glass substrate and are exposed to the ambient atmosphere for some minutes to mount the samples onto the samples holder. The three molecular organic compounds (CoPC, C60-fullerene and F16CuPC) were deposited in situ, i.e. without exposing the organics to the air between thin film preparation and measurement procedures, by PVD (Physical Vapour Deposition) on a Ti substrate (film thickness = appr. 7 nm).

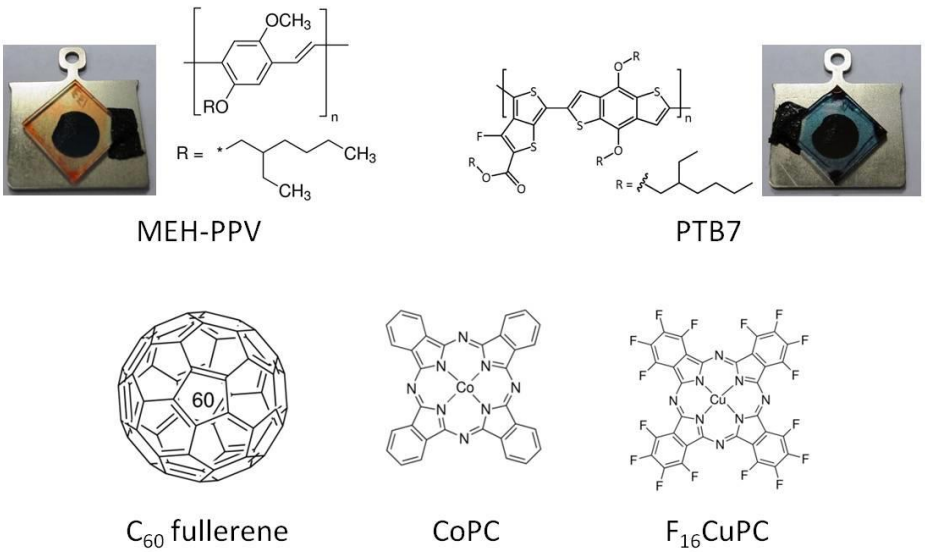

Figure 8: Organic compounds used for the degradation studies

5 Chemical Speciation (XPS)

In the following the chemical change of PTB7 and MEH-PPV thin films is investigated by XPS. For this purpose two degradation experiments were carried out: In the first experiment the polymer thin films were irradiated under absence of ambient atmosphere with unmonochromatized Al-Kα radiation (hν = 1486.6 eV) and in the second experiment the organic thin films are altered by storage for several months under ambient atmosphere. XPS measurements with monochromatized Al-Kα excitation are carried out before and after the degradation procedure.

Figure 9 shows the XPS measurements of the C 1s and O 1s core levels of MEH-PPV before (= pristine thin film) and after two degradation procedures. Because carbon and oxygen are the elements sensitive for XPS in this sample, the C 1s and O 1s core levels representing the complete chemical structure of MEH-PPV. Four components of equal half widths were used to peak fit of the C 1s-XP spectrum for the pristine not-degraded MEH-PPV thin film. The dominant component at *BE* = 284.9 eV represents the sp3-hybridized carbon located in the alkyl moiety "R" (Fig. 8) of MEH-PPV and the component at *BE* = 284.4 eV is attributed to the sp2-hybridized carbon of the polymers backbone. Two components at higher binding energy appear and are assigned to the carbon atoms connected to the adjacent oxygen atoms on side of the aromatic carbon (Csp2, *BE* = 285.6 eV) and of the alkyl moiety (Csp3, *BE* = 286.3 eV). The area ratio between the four components fits well to the formula of the monomer unit of MEH-PPV (Fig. 8). The major component in the O 1s spectrum at *BE* = 532.9 eV represents the oxygen atoms of the aryl alkyl ether in the polymer. The minor components at *BE* = 286.9 eV in the C 1s and at *BE* = 531.3 eV in the O 1s spectrum represent some contaminations in the polymer thin film most likely introduced during the sample mounting under ambient conditions.

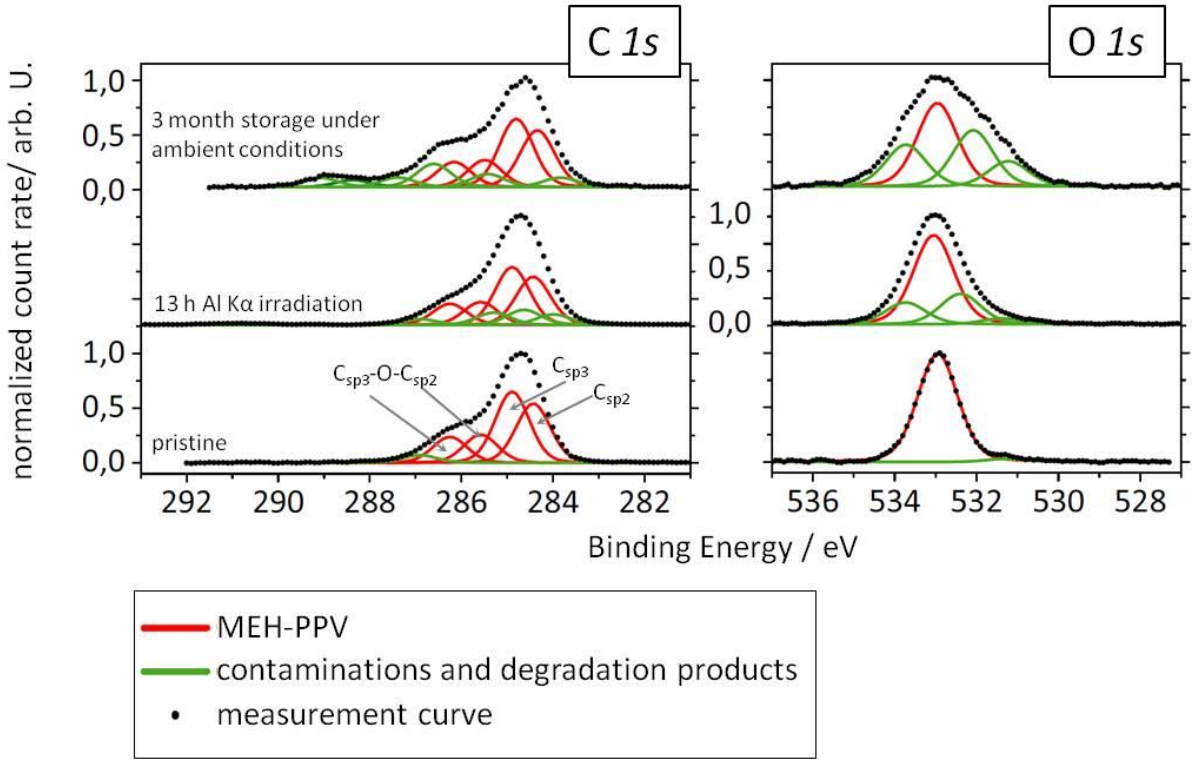

Figure 9: C 1s (left) and O 1s (right) XPS measurements of MEH-PPV thin film before and after the degradation procedures. All spectra are normalized to the maximum and recorded at hν = 1486.6 eV (Al-Kα).

For the peak fit of the C 1s and O 1s XP-spectra of the degraded thin films the parameter sets for the pristine MEH-PPV were used as followed: The *BE* positions, the half widths of the component peaks and the component area ratios (for C 1s) representing the pristine MEH-PPV (red curves in Fig. 7) were constrained or the peak fit of degraded thin films. Additional component peaks were added representing the change of the polymer due to degradation (green curves in Fig. 9).

Regarding to the peak fit, after the 13 h irradiation with Al-Kα photons the three new components appear in the C 1s region at *BE* = 284.0 eV, 284.6 eV and 285.3 eV. Hence, the new components representing the degradation product(s) are distributed over the spectral range between *BE* = 284.0 eV and 285.3 eV where the dominant contributions of the alkyl and sp2-carbon of the pristine polymer appear. Therefore, the majority of the carbon in the degradation products must have a similar chemical environment as the pristine polymer: The low *BE* species at 284.0 eV indicates sp2-hybridized carbon similar to graphene, the component at 284.6 eV is typical for unsaturated carbon with H-atoms and the peak at 285.3 eV is assignable to saturated carbon. Taking the O 1s spectrum into account, it becomes clear, that the oxygen atoms are definitely involved in the degradation process, because two new component peaks appear at *BE* = 532.4 eV and 533.8 eV. Both new species indicate a C-O bond scission in the polymer. The new species at *BE* = 532.4 eV is likely a carboxyl group (C=O).

After the storage of the MEH-PPV thin film for some months under ambient atmosphere, both spectra change significantly. In C 1s region the majority of new species appears at *BE* > 286.6 eV indicating different species of oxidized carbon. The species between *BE* = 286.6 eV and *BE* = 288 eV are assignable to alcohols and carbonyl group containing carbon species (ketones, aldehydes). The

high *BE* species at 289.0 eV corresponds very likely to carboxlic groups (O=C-OH) or carbonates (R-CO3-). Interestingly, a minor component at *BE* = 283.9 eV indicates sp2-hybridized carbon similar to graphene as already generated during the Al-Kα irradiation experiment. The majority of the peak areas in the O 1s region are not assignable to the oxygen of MEH-PPV. New species appear at *BE* = 533.8 eV, 532.2 eV and 531.2 eV. Possible assignments for the 533.8 eV species may be oxygen of an ester (R-O*-C=O) or carboxyl group (HO*-C=O) and sp2-hybridized carbonyl oxygen (O-C=O*, R2C=O*). These assignments are in good agreement with the appearance of the oxidized carbon components in the C 1s spectra.

In the following the two degradation experiments carried out for PTB7 are described. In figure 10 and figure 11 the C 1s, F 1s, S 2p and O 1s core level spectra are shown representing the chemical molecular structure of pristine and degraded PTB7.

The C 1s region of the untreated pristine PTB7 thin film was fitted with six component peaks of equal half widths corresponding to the carbon atoms of different chemical environments in the PTB7 polymer. The ratio between the component-peaks matches very good with the expected values from the molecular formula of the PTB7 monomer. Similar to the corresponding spectrum of MEH-PPV the components at *BE* = 285.1 eV and 284.8 eV represent the carbon atoms of alkyl moieties “R” (Fig. 3) and the sp2-hybridized carbon atoms not connected to sulfur, fluorine or oxygen in the polymer backbone. The components at *BE* = 285.7 eV, 286.5 eV and 287.5 eV are attributed to the sulfur bonded carbon atoms, to Csp2/3-O groups and to Csp2-F. The high oxidized carbon atom of the ester group (RO-C=O) is the component at *BE* = 289.3 eV [Beamson G., Briggs D., High Resolution XPS of Organic Polymers: the Scienta ESCA300 Database, 1992, Unfit 2017 Database, Unfit Scientific GmbH]. F 1s region (Fig. 8, right) exhibits a single peak at *BE* = 687.8 eV characteristic for fluorine substituents of an organic compound [Hoste S., Van De Vondel D.F., Van Der Kelen G.P., . Electron Spectrosc. Relat. Phenom. 17, 191 (1979)] and the S 2p region one doublet at *BE*(S 2p3/2) = 164.3 eV represents aromatic thiophene like sulfur in good agreement with earlier studies [14]. In the O 1s XP-spectrum of the pristine PTB7 thin film the peak fit reveals two component peaks corresponding to C-O-C and O=C-O*R at *BE* = 533.1 eV and to O*=C-OR at *BE* = 532.0 eV.

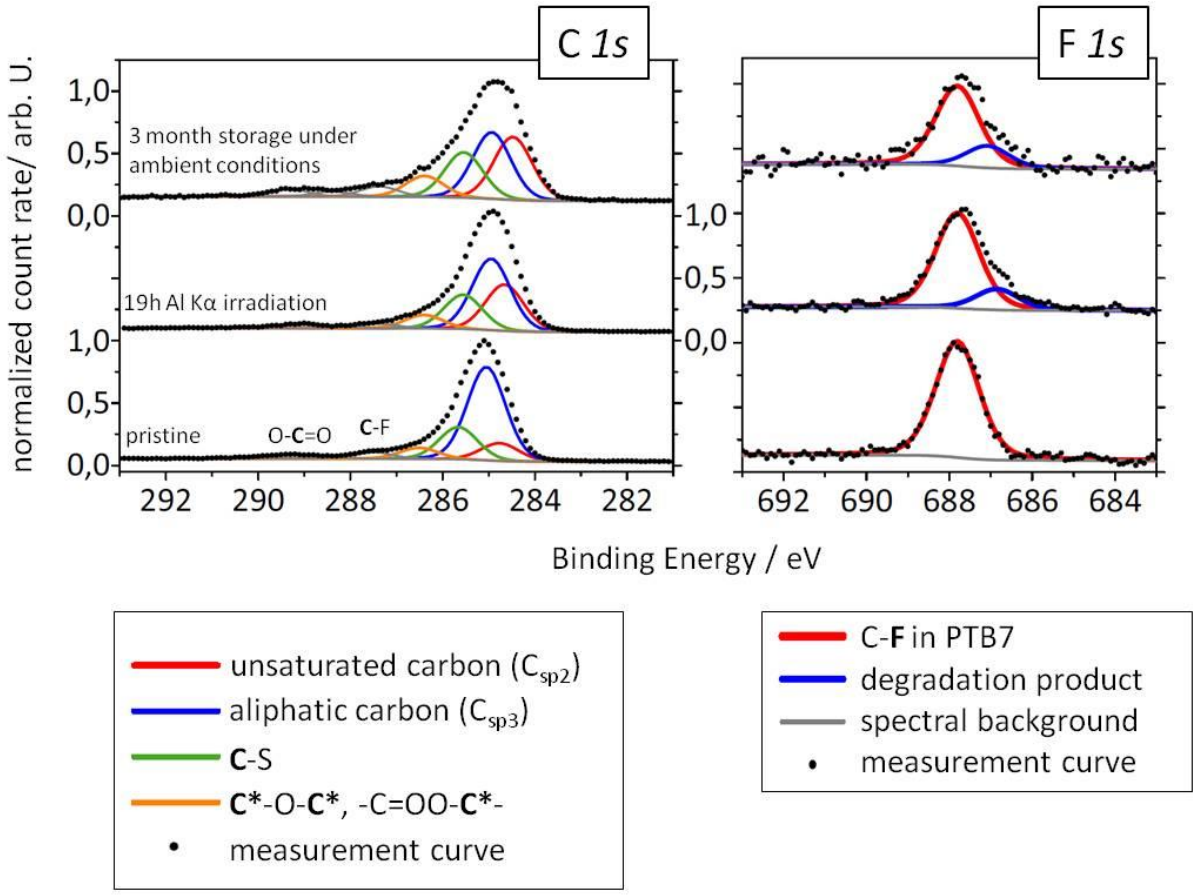

Figure 10: C 1s (left) and F 1s (right) XPS measurements of PTB7 thin film before and after the degradation procedures. C 1s spectra are normalized to the maximum. All spectra were recorded at hν = 1486.6 eV (Al-Kα).

The irradiation of PTB7 by Al-Kα irradiation leads to significant changes in all core level spectra taken into account here. Therefore, all kinds of atoms of the PTB7 structure supposed to be involved in the degradation process. The most prominent change in C 1s region is the increase of the component at *BE* = 284.8 eV revealing a growth of unsaturated carbon, i.e. the change from Csp3- to Csp2-hybridized carbon. Regarding to the molecular structure of PTB7 this degradation process can only occur in alkyl moieties "R" (Fig. 8). A similar interpretation for a degradation effect was already supposed in the last chapter 2.1 where the photons induced degradation was investigated. The F 1s region exhibits that the majority of fluorine substituents remains in the same chemical environment as for the untreated PTB7. Nevertheless, a minor fraction of fluorine changes as can be seen with the new component at *BE* = 686.8 eV. Fluoride ions ("F-") are typically expected at *BE* < 686 eV. Therefore, a C-F bond scission yielding F- ions seems to be improbably. The scission of a CC-bond adjacent to the C-F group is a more feasible assignment for the fluorine degradation product. A slight increase of the component corresponding to carbonyl oxygen (C=O) at *BE* = 532.0 eV is observed in the O 1s region (Fig. 11). Strong changes occurred at the sulfur atoms in the polymer after irradiation indicated by the appearance of a new sulfur species at *BE*(S 2p3/2) = 163.7 eV. This binding energy is still characteristic for organic sulfur not connected to oxygen and/or without a negative charge occurring e.g. in a thiolate group (R-S-). Possible candidates for the new sulfur groups are thiocarbonyl groups (R2C=S), thiols (R-SH) or even disulfides (R-S-S-R) [14].

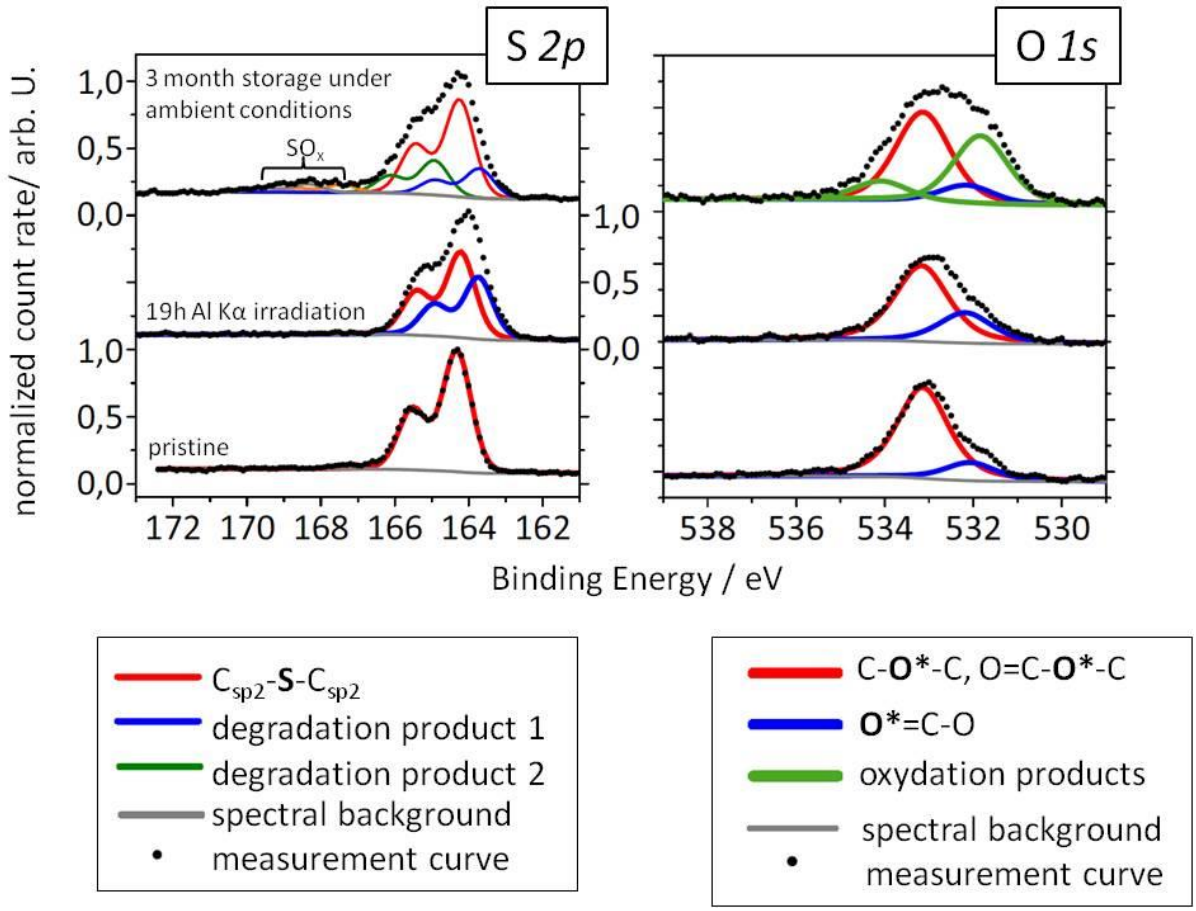

Figure 11: S 2p (left) and O 1s (right) XPS measurements of PTB7 thin film before and after the degradation procedures. S 2p spectra are normalized to the maximum. All spectra were recorded at hν = 1486.6 eV (Al-Kα).

Similar to the results of MEH-PVV, the four core level spectra of PTB7 shows significant changes after storing the thin film(?) for several months under ambient air. C 1s, S 2p and O 1s regions indicate the appearance of oxidation products containing carbon (*BE* > 287.0 eV) or containing sulfur (SOx, *BE*(S 2p3/2) > 165 eV), figures 8 and 9. Interestingly, the degradation under ambient air seems to generate similar degradation effects as observed during the degradation by Al-Kα photons: In the C 1s XP-spectrum a growth of unsaturated carbon is observed at *BE* = 284.8 eV. The F 1s region shows after air and radiation exposure the same effect and the S 2p region exhibits the same degradation product at *BE* = 163.7 eV.

6 Elemental Composition (XPS)

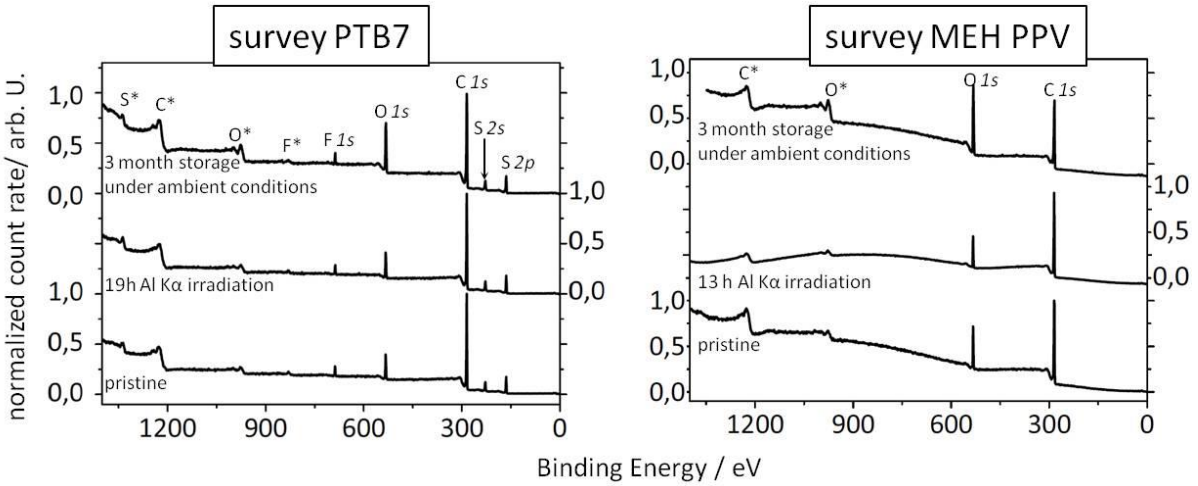

Figure 12: Survey XP-spectra of PTB7 (left) and MEH-PPV (right) thin films before and after the degradation procedures. All spectra were recorded at hν = 1486.6 eV (Al-Kα). The spectral features marked with a star * are assigned to auger transitions of the corresponding element.

In the following the elemental compositions of the polymer thin films before and after the two degradation experiments are mentioned. The survey XP-spectra (Fig. 12) of the pristine polymers exhibit the elements expected from in PTB7 or MEH-PPV and no further contamination of another element. The element ratios (Tab. 1) of the pristine thin films are in good accordance with the values expected from the molecular formula of corresponding monomer unit (Fig. 8). After the irradiations with Al-Kα photons no significant change of the elemental composition of both polymers was observed, which is in good agreement with results of core level spectra discussed in chapter 2.2. The elemental composition changes significantly after the storage of both polymer thin films under ambient atmosphere. An increase of the oxygen amount was observed for both polymers which coincide with the oxidized carbon and sulfur species of the C 1s and S 2p spectra. Further, some minor contaminations were detected after ambient air exposure.

Table 1: Elemental composition of degraded and pristine polymers based on XPS survey spectra of figure 10.

	Elemental concentration / At-%				
	C *1s*	**O *1s***	**S *2p***	**F *1s***	**other**
PTB7					
expected	82	8	8	2	-
pristine	79	10	9	2	-
19 h Al-Kα irradiation	80	9	9	2	-
ambient conditions	74	16	7	2	1 (N)
MEH-PPV					
expected	89.5	10.5	-	-	-
pristine	87	13	-	-	-
13 h Al-Kα irradiation	88	12	-	-	-
ambient conditions	70	28	-	-	2 (N,S,K)

7 Summary

Summarizing the procedures described before the following steps are suggested for Photoelectron spectroscopy on organic semiconductors

1. Sample preparation at best conductive to avoid charging effects
2. Spectra taken at magic angle
3. Calibration of Energy Scale of Photoelectron Spectrometers according to the respective ISO
4. Normalisation at energy position above the electronic structure relevant for the respective spectra
5. Peak fitting procedure with predefined parameters
6. Determination of elemental composition and chemical speciation